Speculations on the Production of Vector Mesons*

S. M. BERMAN AND S. D. DRELL
Stanford Linear Accelerator Center, Stanford University, Stanford, California
(Received 21 August 1963)

Various approximate methods are applied in order to estimate vector boson production at high energies. Most of the calculations refer to photon-induced interactions, but in addition a certain class of reactions induced by π and K beams is discussed. The photoproduction of ρ's and ω's is considered by a diffraction mechanism as well as by a one-pion-exchange mechanism. Both of these methods lead to surprisingly large numbers for the cross section. The subsequent decay of $\rho^0(\omega^0) \to e^+(\mu^+)+e^-(\mu^-)$ is considered as a possible and interpretable correction to the pure quantum electrodynamic calculations of large angle pair production. The possibility of measuring the $\rho(\omega)\pi\gamma$ coupling constant is examined by considering the coherent process in the nuclear Coulomb field $\pi+A \to \rho(\omega)+A$. The question of whether vector boson production could give significant enhancement to secondary pion and kaon beams is considered. No confident theoretical statement can be made about this question, and a definite answer depends on the experimental determination of certain parameters.

I. INTRODUCTION

A NUMBER of high-energy processes are computed in terms of observed strong interaction cross sections. We are concerned here primarily with photon initiated reactions but consider in addition a class of related π and K beam interactions.

It is neither the aim nor pretension of these calculations to yield quantitatively reliable results. Quite the contrary; we are fully aware of the very crude nature of the approximations and intend the results only to show those special features which may be of value in planning experiments at the new accelerators.

We suspect that many of these results may be found in the lower left-hand drawer of the desks of many of our colleagues; however, we feel it of some value to compile these results in one place.

We consider first, in Secs. II and III, the cross sections to photoproduce the ρ^0 and ω as unstable heavy brothers of the photon via diffraction and one-pion-exchange channels. From our estimates it appears feasible to detect their rare electromagnetic decay modes ρ^0, $\omega \to e^+ + e^-$ and ρ^0, $\omega \to \mu^+ + \mu^-$ and thereby to confront quantum electrodynamics with new tests.

In arriving at these results it is necessary to introduce interaction vertices for the ρ and ω resonances with pions and photons and to appeal to existing experimental numbers. The possibility of directly measuring some of these parameters by observing coherent production of vector resonances from incident π's (or K's) in a nuclear Coulomb field is discussed in Sec. IV. For some parameters we must appeal to theoretical arguments as given by Gell-Mann and Zachariasen[1] who discussed the dispersion theoretic basis for a model introducing the vector resonances into diagrams with elementary couplings. Those discussions and the subsequent work of Gell-Mann, Sharp, and Wagner[2] are extended in Sec. II to further reactions at higher energies.

In Sec. V we consider possible photoproduction amplitudes involving absorption of the incident photon on the currents of the vector resonances. Finally in Sec. VI we compare the various channels as production mechanisms for secondary π and K beams from photon accelerators.

It is to be understood that questions of "elementarity" versus "dynamical resonance" of the vector bosons are of no concern here. The plan is a purely phenomenological one of relating different processes which proceed through common interaction vertices and channels.

II. DIFFRACTION PRODUCTION

The first class of processes we consider proceeds via a diffraction channel. A photon materializes via diffraction scattering from a proton target, say, as a spin-one resonance with the same quantum numbers as a γ: $J=1$; parity $P=-1$; $I=1$, 0; charge conjugation $C=-1$. This process is recognized by observing a bump in the decay spectrum at the resonance mass and by recognizing a diffraction angular distribution similar to the observed pattern in $\pi-N$ and $N-N$ scattering at the same total energy $s=(p_1+p_2)^2=[E_{\text{c.m.}}^{\text{tot}}]^2$. The first question to answer is: what are the vector resonances coupled to the photon; i.e., what bumps are found in the mass spectrum in addition to the ρ and $\omega(\varphi)$ at 750 and 780 MeV, respectively? If the soft cores in the electromagnetic form factors[3] are to be associated with heavy vector resonances with $m^* \approx 1 \cdot 1$ BeV, they should be observed via their primary decay channels.

In order to estimate the cross section for this process we turn to the Amati, Fubini, Stanghellini[4] model of diffraction scattering to relate the $\gamma \to$ vector diffraction cross section to observed π and N diffraction measurements.

* Supported by the U. S. Atomic Energy Commission.
[1] M. Gell-Mann and F. Zachariasen, Phys. Rev. 124, 953 (1961).
[2] M. Gell-Mann, R. Sharp, and W. Wagner, Phys. Rev. Letters 8, 261 (1962).
[3] L. Hand, D. G. Miller, and R. Wilson, Rev. Mod. Phys. 35, 335 (1963).
[4] D. Amati, S. Fubini, and A. Stanghellini, Nuovo Cimento 5, 896 (1962).

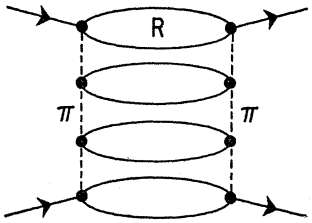

FIG. 1. Rung diagram describing Amati, Fubini, and Stanghellini model of diffraction scattering.

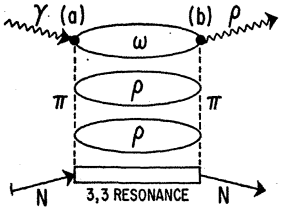

FIG. 3. Rung diagram for photoproduced ρ^0 via diffraction mechanism.

In this model diffraction scattering is calculated by summing over-all two-pion-exchange graphs as in Fig. 1. Each rung in the ladder represents a low-energy-resonant $\pi\pi$ system (a πN system for the top and bottom rungs in NN scattering and for the bottom rung in πN scattering) and the sum of these graphs for all numbers of rungs in the ladders represents an *approximate* solution for the elastic amplitude in the strip approximation to the Mandelstam representation.[5] The absorptive part of the amplitude proceeding through real intermediate resonant states dominates.

In application so far this model has been limited to point S-wave couplings where it has the now uncertain virtue of leading to the Regge-pole behavior of a diffraction pattern of shrinking width with increasing energy. We use it here only to estimate *ratios* of diffraction cross sections in the following way. The ratio of NN to πN diffraction scattering is given by the ratio of πN resonance to $\pi\pi$ resonance couplings as in Fig. 2. Treating the virtual exchanged pion as an incident real one at the top vertices, forming a 33 resonance in the NN-scattering case and a ρ resonance in the πN case, with the resonance propagating on the mass shell (absorptive amplitude) we find

$$\left\{\frac{d\sigma_{NN}(s,t)/dt}{d\sigma_{\pi N}(s,t)/dt}\right\}_{s/t>>1,t\to 0}\approx\frac{(d\sigma_{33}(\omega_r,\,t=0)/dt)}{(d\sigma_{\pi\pi,\rho}(\omega_\rho,\,t=0)/dt)}\approx(1.3)^2,$$

which is close to the observed ratio, by the optical theorem, of

$$\{\sigma_{NN}{}^{\rm tot}(s)/\sigma_{\pi N}{}^{\rm tot}(s)\}^2\approx(40\text{ mb}/27\text{mb})^2.$$

Similarly for the photoproduction of a ρ meson, say, in the forward direction we consider the diagram Fig. 3 in the spirit of the AFS model and evaluate it in terms

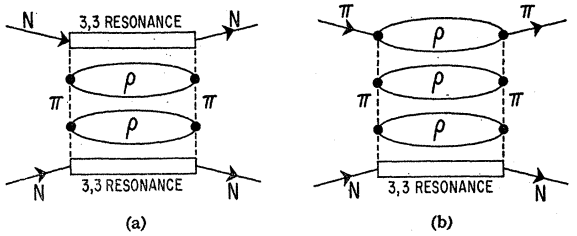

FIG. 2. Rung diagrams for diffraction scattering. (a) nucleon-nucleon; (b) pion-nucleon.

[5] D. Amati, S. Fubini, A. Stanghellini, and M. Tonin, Nuovo Cimento 22, 569 (1961).

of the *observed* π-nucleon diffraction cross sections by evaluating the ratio of the vertices at the top rungs in the ladder in Figs. 2(b) and 3 in the resonance region.

In calculating the $\pi-N$ scattering amplitude we introduce a $\rho\pi\pi$ coupling

$$g_{\rho\pi\pi}\epsilon_\mu(\rho)[k_1+k_2]^\mu \tag{1}$$

at a vertex in Fig. 2(b) to form the ρ resonance in the $\pi\pi$ interaction. The kinematics are illustrated in Fig. 4, and the coupling constant $g_{\rho\pi\pi}$ is determined from the measured width of the dominant 2π decay mode of the ρ

$$\Gamma_\rho=\frac{1}{12}\left(\frac{g_{\rho\pi\pi}{}^2}{4\pi}\right)\left\{1-\frac{4m_\pi{}^2}{m_\rho{}^2}\right\}^{3/2}m_\rho. \tag{2}$$

With this interaction we obtain for forward scattering of the incident π meson at the top rung of Fig. 2(b)

$$\begin{aligned}-g_{\rho\pi\pi}{}^2(k+q)_\mu\left[g^{\mu\nu}-\frac{(k-q)^\mu(k-q)^\nu}{m_\rho{}^2}\right](k+q)_\nu&\\ =-g_{\rho\pi\pi}{}^2\left[(k+q)^2-\frac{(k^2-q^2)^2}{m_\rho{}^2}\right]&\\ =g_{\rho\pi\pi}{}^2m_\rho{}^2[1+O(m_\pi{}^2/m_\rho{}^2)],&\end{aligned} \tag{3}$$

where the kinematics is taken as illustrated in Fig. 5, and we make the peripheral approximation $|q^2|\approx m_\pi{}^2\ll m_\rho{}^2$.

In calculating the ρ photoproduction we must introduce $\gamma\pi\omega$ and $\rho\pi\omega$ vertices at (a) and (b) in Fig. 3. These have unique gauge invariant forms with factors

$$\frac{g_{\gamma\pi\omega}}{m_\rho}\epsilon_{abcd}\epsilon^a(\gamma)k^b(\gamma)\epsilon^c(\omega)k^d(\omega) \tag{4}$$

and

$$\frac{g_{\rho\pi\omega}}{m_\rho}\epsilon_{abcd}\epsilon^a(\rho)k^b(\rho)\epsilon^c(\omega)k^d(\omega) \tag{5}$$

corresponding to kinematics as shown in Fig. 6.

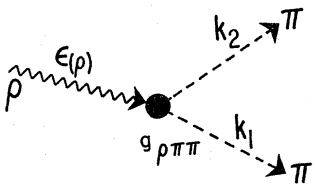

FIG. 4. The $\rho\pi\pi$ vertex; k_1 and k_2 are the four momenta of the pions and $\epsilon(\rho)$ is the ρ polarization vector.

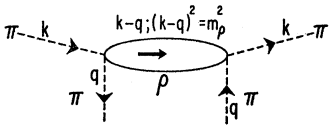

FIG. 5. Top rung of pion-nucleon diffraction scattering diagram. The intermediate ρ of momentum $(k-q)$ is shown by the two lines.

A relation between the two coupling constants in (4) and (5) is given in Ref. 1 on the basis of a universal coupling scheme for vector mesons[6]:

$$g_{\gamma\pi\omega}=\frac{e}{2\gamma_\rho}g_{\rho\pi\omega}. \tag{6}$$

The ρ and ω may be substituted for each other every-

[6] In this model the vector ρ and ω mesons couple to photons with a direct coupling $(e/2\gamma_V)m_V^2\epsilon(\gamma)\cdot\epsilon(V)$ and the constants are related by $g_{\gamma\pi\omega}=g_{\rho\pi\omega}e/2\gamma_V$. This coupling is not explicitly gauge invariant. As introduced here it is not more than a formal statement of the approximation that the dominant electromagnetic interactions proceed via the resonant 2π state with $I=1$ (ρ meson) or 3π state with $I=0$ (ω meson). The propagator of the ρ (or ω) coupling the virtual photon to a nucleon line gives the approximately observed electromagnetic form factor dependence. To nucleons the $I=1$ vector meson (ρ) couples the conserved isovector current

$$g_{\rho NN}\bar{u}(f)\boldsymbol{\tau}\left[\gamma^\mu+\frac{iK_V}{2M}\sigma^{\mu\nu}q_\nu\right]u(i)\hat{\varphi}_\rho\epsilon_\mu(\rho),$$

where $\hat{\varphi}_\rho$ denotes a unit isovector for the ρ isotopic triplet; and $K_V=1.85$ is the observed anomalous isovector moment; the ω couples to the isoscalar current

$$g_{\omega NN}\bar{u}(f)\left[\gamma^\mu+\frac{iK_S}{2M}\sigma^{\mu\nu}q_\nu\right]u(i)\epsilon_\mu(\omega),$$

where $K_S=-0.06$ is the isoscalar moment. No form factors $F(q^2)$ are introduced to modify significantly the point couplings for varying q^2 values. The observed q^2 dependence of the electromagnetic form factors of nucleons comes from the vector boson propagators joining photons onto the nucleon line. This gives for the isovector interaction for example

$$\left(\frac{eg_{\rho NN}}{2\gamma_\rho}\right)\left[\frac{(-m_\rho^2)\epsilon_\mu(\gamma)}{q^2-m_\rho^2+i\Gamma_\rho m_\rho}\right]\bar{u}(f)\left[\gamma^\mu+\frac{iK_V}{2M}\sigma^{\mu\nu}q_\nu\right]\boldsymbol{\tau}\cdot\hat{\varphi}_\rho u(i).$$

The common Dirac and Pauli form factor dependence on q^2 is then

$$F_V(q^2)=\frac{g_{\rho NN}}{\gamma_\rho}\left[1-\left(\frac{q^2}{m_\rho^2}\right)-\left(\frac{i\Gamma_\rho}{m_\rho}\right)\right]^{-1}$$

where the imaginary term has meaning only near the resonance $q_r^2=m_\rho^2$ for time-like momenta. The ratio of constants $g_{\rho NN}/\gamma_\rho$ measures the importance of the ρ channel in the observed electromagnetic structure. If the entire interaction proceeds via the ρ channel the ratio would be $g_{\rho NN}/\gamma_\rho=1$ corresponding to a universal coupling scheme. A closer approximation to experiment (see Ref. 3) is obtained with $g_{\rho NN}/\gamma_\rho\approx 2$ and, for $0>q^2>-3m_\rho^2$

$$F_V(q^2)\approx\frac{2}{1-q^2/m_\rho^2}-\frac{1}{1-q^2/2m_\rho^2}.$$

A similar form is consistent with observation of the isoscalar form factor. See Ref. 3 for accurate parameters.

In the present applications there are no worries about gauge invariance due to the form assumed above for the direct $(\gamma-\rho)$ and $(\gamma-\omega)$ couplings. The electromagnetic interaction will be only to conserved currents if the ω and ρ channels through which it proceeds couple only to conserved hypercharge and isotopic currents, respectively. No false static charge couplings are possible in this case. For example, a cancellation between ρ and ω assures that the neutron has zero static charge. For the hyperons there is no $\gamma\to\omega\to\Lambda$ coupling since the Λ hypercharge vanishes, and for neutral Σ vertices $\gamma\to\rho\to\Sigma^0$ also vanishes. The only practical use made here of this interaction is in relating the $\pi\rho\omega$ coupling constant $g_{\rho\omega\pi}$ in Eq. (5) to observable $(\pi\omega\gamma)$ and $(\pi\rho\gamma)$ coupling strengths on one hand and to the $\pi^0\to 2\gamma$ decay rate as estimated by Gell-Mann *et al.* (Ref. 2).

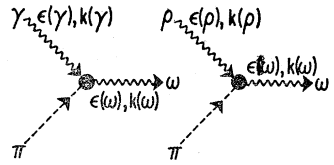

FIG. 6. The $\omega\gamma\pi$ vertex and the $\omega\rho\pi$ vertex, respectively.

where in (4), (5), and (6). A crude estimate of γ_ρ and γ_ω may be made by assuming the ρ and ω channels to dominate the nucleon and pion electromagnetic form factors completely, so that

$$g_{\rho\pi\pi}=2\gamma_\rho=2\gamma_\omega, \tag{7}$$

where the last equality assumes unitary symmetry and the factors of two relative to Ref. 2 are in the definition of the γ's. From (2) we find $g_{\rho\pi\pi}^2/4\pi\approx 2$ for $\Gamma_\rho\approx 100$ MeV [7] and therefore

$$(\gamma_\rho^2/4\pi)\approx(\gamma_\omega^2/4\pi)\approx\tfrac{1}{4}(g_{\rho\pi\pi}^2/4\pi)\approx\tfrac{1}{2}; \tag{8}$$

$$(g_{\gamma\pi\omega}^2/4\pi)\approx g_{\gamma\pi\rho}^2/4\pi\approx\tfrac{1}{2}\alpha(g_{\rho\pi\omega}^2/4\pi). \tag{9}$$

A crude estimate of the magnitudes of the coupling constants in (9) is given in Ref. 2 in terms of a model of the $\pi^0\to 2\gamma$ decay via Fig. 7. The decay rate, in the present notation, is

$$\tau_{\pi^0}^{-1}\equiv\Gamma_{\pi^0}=\frac{1}{64}\alpha^2\frac{m_\pi^3}{m_\rho^2}\frac{(g_{\rho\pi\omega}^2/4\pi)}{(\gamma_\rho^2/4\pi)(\gamma_\omega^2/4\pi)} \tag{10}$$

and from the measured rate of[8]

$$\tau_{\pi^0}^{-1}\approx 1\times 10^{16}\ \text{sec}^{-1}\approx 6\ \text{eV}.$$

we find

$$\frac{(g_{\rho\pi\omega}^2/4\pi)}{(\gamma_\rho^2/4\pi)(\gamma_\omega^2/4\pi)}\approx 1.5,\quad\text{or}\quad\left(\frac{g_{\rho\pi\omega}^2}{4\pi}\right)\approx 0.4, \tag{11}$$

and

$$g_{\gamma\pi\omega}^2/4\pi\approx g_{\gamma\pi\rho}^2/4\pi\approx\tfrac{1}{5}\alpha. \tag{12}$$

Alternatively we may appeal to the bootstrap calculation of Zachariasen and Zemach[9] for the estimate

$$g_{\rho\pi\omega}^2/4\pi\approx 2\text{ to }4. \tag{13}$$

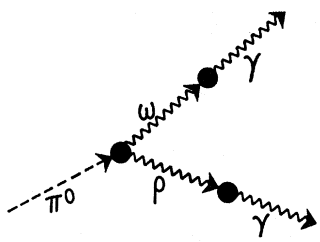

FIG. 7. π^0 decay in two photons via intermediate ρ and ω poles.

[7] J. Button, G. Kalbfleisch, G. Lynch, B. Maglić, A. Rosenfeld, and M. Stevenson, Phys. Rev. **126**, 1858 (1962); D. O. Caldwell, E. Bleuler, B. Elsner, L. W. Jones, and B. Zacharov, Phys. Letters **2**, 253 (1962).

[8] G. von Dardel, D. Dekkers, R. Mermod, J. Van Putten, M. Vivargent, F. Weber, and K. Winter, Phys. Letters **4**, 51 (1963).

[9] F. Zachariasen and A. C. Zemach, Phys. Rev. **128**, 849 (1962).

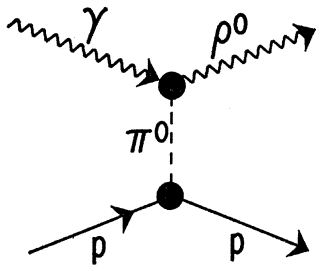

FIG. 8. ρ^0 photoproduction via one-pion-exchange mechanism.

The constants $g_{\rho\pi\gamma}^2/4\pi$ and $g_{\omega\pi\gamma}^2/4\pi$ can then be related to peripheral photoproduction cross sections or measured as discussed in Sec. IV for $\rho^\pm$ production from $\pi^\pm$ in a Coulomb field. They are expressed in terms of $\Gamma_{\rho(\omega)\to\pi+\gamma}$, the partial width for the process $\rho(\omega)\to\pi+\gamma$ by

$$\Gamma_{\rho(\omega)\to\pi\gamma}=\frac{1}{24}\left(\frac{g_{\rho(\omega)\pi\gamma}^2}{4\pi}\right)m_\rho\left(1-\frac{m_\pi^2}{m_\rho^2}\right)^3. \quad (14)$$

In the experiment of McLeod, Richert, and Silverman,[10] a ρ^0 bump appears in the reaction $\gamma+p\to p+\pi^+ +\pi^-$ for an incident photon energy of ≈ 1 BeV. If this bump is analyzed in terms of a one-pion-exchange peripheral production as in Fig. 8, one finds

$$\Gamma_{\rho\to\pi\gamma}\approx 0.5 \text{ MeV}$$

or, by (14)

$$(g_{\rho\pi\gamma}^2/4\pi)\approx 0.016. \quad (15)$$

This is one order of magnitude larger than the result suggested in (12). The value (15) may be grossly in error since all nonpole contributions were excluded in analyzing the ρ bump in the experiment of McLeod *et al.* However, at the energy of 1 BeV the distance of the physical region from the one-pion pole ($>m_\rho^2/2k \approx 300$ MeV) is large enough so as not to encourage optimism in the quantitative meaning of this approximation. In Sec. IV we propose an experiment measuring $\Gamma_{\rho\pi\gamma}$ directly but for present work take (12) and (15) as lower and upper limits, respectively.[11]

With the interactions (4) and (5) we compute, after some algebra for the forward scattering of a γ to a ρ at the top rung of Fig. 3,

$$(g_{\gamma\pi\omega}g_{\rho\pi\omega}/m_\rho^2)\boldsymbol{\varepsilon}\cdot\boldsymbol{\varepsilon}_\rho[\tfrac{1}{2}m_\rho^2 q^2+\tfrac{1}{4}m_\rho^2\bar{q}^2 -\tfrac{1}{4}q^2\bar{q}^2+\tfrac{1}{4}m_\rho^2|\mathbf{q}_\perp|^2] \quad (16)$$

where the kinematics is shown in Fig. 9; $|\mathbf{q}_\perp|$ denotes

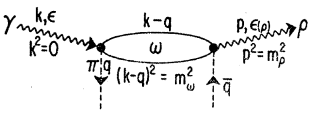

FIG. 9. Top rung of photoproduced ρ-diffraction diagram.

the transverse part of the momentum components of the intermediate π mesons: $\mathbf{q}_\perp\cdot\mathbf{k}=0$. In the AFS model the π meson propagating with q, after forming the first resonance $(k-q)^2=m_\omega^2$, retains almost all of the incident energy k and is very relativistic. From this and the momentum transfer in the laboratory system, $m_\rho^2/2k_0$, required to form the ρ in the forward direction it follows that

$$\bar{q}^2-q^2\approx m_\rho^2.$$

Therefore, both intermediate mesons cannot be near their mass shells simultaneously. For a rough estimate we take $q^2\approx 0$ and find for (16)

$$(g_{\gamma\pi\omega}g_{\rho\pi\omega})\boldsymbol{\varepsilon}_\rho\cdot\boldsymbol{\varepsilon}[\tfrac{1}{4}m_\rho^2].$$

Combining with Eq. (3) we arrive at

$$\left(\frac{d\sigma(st)}{d\Omega}\right)_{\gamma+p\to p+\rho,\ \text{diffraction},\ \theta\to 0} =\left(\frac{1+\cos^2\theta}{2}\right)\frac{p_\rho}{E_\rho}\left(\frac{1}{4}\right)^2\frac{[g_{\gamma\pi\omega}^2/4\pi][g_{\rho\pi\omega}^2/4\pi]}{[12\Gamma_\rho/m_\rho]^2} \times\left(\frac{d\sigma(st)}{d\Omega}\right)_{\pi N,\ \text{diffraction},\ \theta\to 0}. \quad (17)$$

We shall consider numerical results in more detail later but here we note that additional contributions to the absorptive amplitude come from the π current which contributes to a diagram like Fig. 10. This contribution is neglected here and if important would serve only to *enhance* our predicted cross sections since absorptive amplitudes are always positive.[12]

From this model of converting incident γ rays into massive vector bosons via a diffraction scattering a number of specific predictions follow. The numerical values of cross sections are not to be considered to carry great significance but the indicated qualitative behaviors are presented as motivation for experimental searches.

The $\rho^0(\omega^0)$ angular distribution and the energy variation of the cross section should follow the general features of elastic diffraction cross sections as observed in πN and NN scattering. Furthermore, the vector bosons are transversely polarized as are the incident photons. Thus, the angular distribution of one of the final pions in the $\rho\to 2\pi$ decay will be $\sin^2\theta_D$ about the

[10] D. McLeod, S. Richert and A. Silverman, Phys. Rev. Letters **7**, 383 (1961).

[11] One may also attempt to determine $\Gamma_{\rho\pi\gamma}$ and $\Gamma_{\omega\pi\gamma}$ from the ρ and ω exchange poles in single-pion photoproduction. Here one has the difficulty that the retardation denominators for these heavier mass vector mesons are difficult to identify, and furthermore considerable mystery still shrouds the ρ and ω exchange channels in high-energy amplitudes. See R. Talman, C. Clinesmith, R. Gomez, and A. Tollestrup, Phys. Rev. Letters **9**, 177 (1962); H. Palevsky, J. Moore, R. Stearns, H. Meuther, R. Sutter, *et al.* Phys. Rev. Letters **9**, 509 (1962); S. D. Drell, in *Proceedings of the International Conference on High Energy Physics*, edited by J. Prentki (CERN, Geneva, 1962), p. 897.

[12] The amplitude for Fig. 10 is very difficult to estimate without a detailed theory since the transverse polarization of the incident photon and angular momentum conservation along the incident axis require a nonvanishing transverse momentum of the intermediate π.

incident photon direction as viewed in the rest system of the ρ resonance.

If this mechanism of $\rho^0(\omega^0)$ production is sufficiently copious it provides the possibility of observing the rare decay branching ratios $\rho^0, \omega^0 \to e^+, e^-$ and μ^+, μ^-. From the ratio of these two decay branches one has the very attractive possibility of comparing muon and electron electrodynamic vertices for time like momenta of ≈ 750 MeV, as already noted by many authors.[13]

With this aim consider the photoproduction of charged lepton pairs ($\mu^+\mu^-$ or e^+e^-) through the diffraction scattering of the γ into ρ or ω. The diagrams considered are shown in Fig. 11.

The encircled mechanism of the ω^0, ρ^0 decay to a lepton pair is that of Gell-Mann *et al.*[2,6] and corresponds to a decay rate of

$$\Gamma_{V\to ll}=\frac{\alpha^2}{(\gamma_V^2/4\pi)}\frac{m_V}{12}\left\{1+0\left(\frac{m_l^4}{m_V^4}\right)\right\}$$
$$\approx 3 \text{ keV}$$
$$\approx 3\times 10^{-5}\times\Gamma_{\rho\to 2\pi}. \tag{18}$$

Alternatively we may view the processes in Fig. 11 as Compton scattering of a real photon with $k^2=0$ to a virtual photon with $s=p^2=(l_+ + l_-)^2\approx m_\rho^2>0$. The form factor at the vertex from which the virtual photon emerges is given, near the ρ, ω mass by a propagator $(s-m_V^2+i\Gamma_V m_V)^{-1}$ as discussed in footnote 6 in analogy to the nucleon electromagnetic form factor discussions. This point of view leads to the same result as does (18). For the lepton pair produced symmetrically about the forward direction, with

$$k\cdot p_+ = k\cdot p_- \approx kE(1-\beta_\rho\cos\theta);$$
$$E\equiv E_+ = E_-(\approx k/2),$$

this contribution does not interfere with the ordinary Bethe-Heitler pair production amplitude[14] and the cross section is ($m_\rho = m_\omega$ except in the resonance denominators and the mass of the lepton is neglected, i.e., $m_l^2/m_\rho^2 \ll 1$)

$$\frac{d\sigma_{\gamma\to l+\bar{l}}}{d\Omega_+ d\Omega_- d\epsilon_+}$$
$$=\frac{1}{2}\frac{(g_{\omega\pi\rho}^2/4\pi)(g_{\gamma\pi\rho}^2/4\pi)}{(8\pi)^4}\frac{[12\Gamma_{\omega\to l\bar{l}}/m_\rho]}{[12\Gamma_\rho/m_\rho]^2}m_\rho^2 k^3$$
$$\times[\sigma_{\pi N}^{\text{tot}}(s)]^2\left|\frac{1}{s-m_\omega^2+i\Gamma_\omega m_\omega}\right.$$
$$\left.+\left\{\frac{\gamma_\omega^2/4\pi}{\gamma_\rho^2/4\pi}\right\}\frac{1}{s-m_\rho^2+i\Gamma_\rho m_\rho}\right|^2, \tag{19}$$

[13] See, for example, Ref. 2 and the *Proceedings of the International Conference on High Energy Physics*, edited by J. Prentki (CERN, Geneva, 1962).

[14] J. Bjorken, S. D. Drell, and S. Frautschi, Phys. Rev. **112**, 1409 (1958).

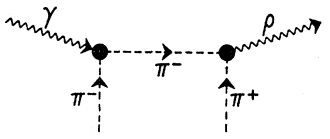

FIG. 10. Top rung of a possible diagram contributing to the absorptive amplitude in the photoproduction of ρ^0.

where $s\equiv(p_+ + p_-)^2$ is the mass of the ρ or ω state formed and we are interested for s near the resonance at $\approx m_\rho^2$. Introducing (6), (10), and (18) into (19) and expressing the result as a ratio to the Bethe-Heitler formula for the same energies and angles we find

$$R=\frac{(d\sigma/d\Omega_+ d\Omega_- d\epsilon_+)_{\text{Diffraction}}}{(d\sigma/d\Omega_+ d\Omega_- d\epsilon_+)_{\text{Bethe-Heitler}}}=\frac{1}{128}\frac{\tau_{\pi^0}^{-2}}{\alpha^4}\frac{m_\rho^{12}}{m_\pi^{10}}\left(\frac{m_\rho}{12\Gamma_\rho}\right)^2$$
$$\times\left|\frac{\gamma_\omega^2}{4\pi}\frac{1}{s-m_\rho^2+i\Gamma_\rho m_\rho}+\frac{\gamma_\rho^2}{4\pi}\frac{1}{s-m_\omega^2+i\Gamma_\omega m_\omega}\right|^2. \tag{20}$$

Inserting the experimental lifetime (11) and the observed $\rho\to 2\pi$ decay width $\Gamma_\rho\approx 100$ MeV into (20) we arrive at the ratio

$$R\approx 2\times 10^{-3}\left|\frac{\gamma_\omega^2}{4\pi}\frac{1}{1-s/m_\rho^2-i\Gamma_\rho/m_\rho}\right.$$
$$\left.+\frac{\gamma_\rho^2}{4\pi}\frac{1}{1-s/m_\omega^2-i\Gamma_\omega/m_\omega}\right|^2. \tag{21}$$

Alternatively an estimate based on (13), (15), and (18) gives a ratio R' larger than Eq. (21) by a factor of ≈ 10:

$$R'\approx 30R. \tag{22}$$

Finally this ratio varies with the measured decay width of the $\rho\to 2\pi$ roughly as $\approx 1/\Gamma_\rho^3$ and is therefore further increased by the smaller width reported in the high-energy measurements.[7]

These results (21) and (22), while numerically unreliable are neither sufficiently large nor small that one can say for certain that there will or will not be an observable bump in the mass spectrum of lepton pairs

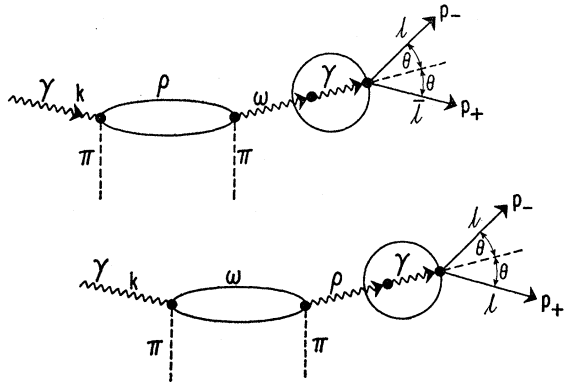

FIG. 11. Diagram showing ρ and ω photoproduced by diffraction mechanism and subsequently decaying into lepton pairs.

at $s\approx m_\rho^2$. With a resolution width $<\Gamma_\rho/2$ in detecting the mass of the $l\bar{l}$ pair they lead to ratios spanning unity at $s=m_\rho^2$. Off resonance $R\ll 1$ and, in particular, for $s<m_\rho^2$, $R<10^{-2}$. This is because the diffraction channel decreases as we move below resonance whereas the Bethe-Heitler formula for large angle pair formation increases according to $1/s^3$ as the mass of the lepton pair decreases for a fixed incident γ energy.

Equations (21) and (22) constitute a possible and interpretable correction to the pure electrodynamic calculations of large angle pair formation.[14] Great interest in observing a bump in the lepton mass spectrum comes from the fact that the ratio of bumps at $s\approx m_\rho^2$ for $\mu^+\mu^-$ to e^-e^+ pair production must be one (to within an accuracy of $\approx m_\mu^2/m_\rho^2<2\%$) if the μ and e have the same electrodynamic interactions. Any deviation of this ratio from unity would be a manifestation of a difference in the electromagnetic vertices of the muon and electron for time-like momenta of $\approx s\approx$ (780 MeV)^2. The possibility of such differences is not ruled out by any present experimental information, and therefore, a bump in the lepton pair spectrum at $s\approx m\rho^2$ would be of great interest to observe.

III. ONE-π-EXCHANGE AMPLITUDES

We consider next the production of ρ or ω mesons in the one-pion-exchange model. Pions are assumed to be coupled to γ and $\rho(\omega)$ by a coupling of the form of Eq. (4). In addition to elastic ρ^0 and ω production from nucleons,

$$\gamma+p\rightarrow\rho(\omega)+N \tag{23}$$

as in Fig. 8, one-π exchange also leads to charged bosons and to excitations of the various possible $\pi-N$ states

$$\gamma+p\rightarrow\rho(\omega)+N^* \tag{24}$$

denoted by N^* in (24) and in Fig. 12.

The laboratory differential cross section for (23) in the one-pion-exchange approximation, neglecting any form factor associated with the pion propagator, the $\gamma\pi\rho(\omega)$ vertex and the πNN vertex is

$$\left(\frac{d\sigma}{d\Omega}\right)_{\rm lab}=\left(\frac{g_{\pi NN}{}^2}{4\pi}\right)\left(\frac{\Gamma_{\rho(\omega)\rightarrow\pi\gamma}}{m_{\rho,\omega}}\right)\frac{|t|}{m_{\rho,\omega}{}^2}\left(\frac{3p^2}{2k^2}\right)\times\left\{\frac{|t|+m_{\rho,\omega}{}^2}{|t|+m_\pi{}^2}\right\}^2\frac{1}{M^2B_1}, \tag{25}$$

where $|t|$ is the invariant momentum transfer, $k=$ incoming photon energy, $M=$ nucleon mass, $g_{\pi NN}{}^2/4\pi\approx 14$; $\Gamma_{\rho(\omega)\rightarrow\pi\gamma}$ is given in Eq. (14), $p=$ momentum of outgoing ρ meson, and

$$MkB_1=[(Mk+\tfrac{1}{2}m_{\rho,\omega}{}^2)^2-m_{\rho,\omega}{}^2\{(M+k)^2-k^2\cos^2\theta\}]^{1/2}, \tag{26}$$

where θ is the $\rho(\omega)$ production angle.

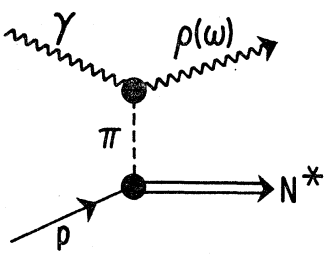

FIG. 12. ρ^0N^* photoproduction via one-pion-exchange mechanism.

In the forward direction and in the limit where $m_{\rho,\omega}/k\ll 1$ and $|t_{\rm min}|^{1/2}=m_{\rho,\omega}{}^2/2k\ll m_\pi$, we have for ρ^0 production (multiply by 2 for $\rho^\pm$)

$$\left(\frac{d\sigma}{d\Omega}\right)_0=\frac{3}{8}\left(\frac{g_{\pi NN}{}^2}{4\pi}\right)\left(\frac{\Gamma_{\rho(\omega)\rightarrow\pi\gamma}}{m_{\rho,\omega}}\right)\left(\frac{m_{\rho,\omega}}{M}\right)^2\left(\frac{m_{\rho,\omega}}{m_\pi}\right)^4\frac{1}{k^2}. \tag{27}$$

Using (15) for a numerical estimate we find

$$(d\sigma/d\Omega)_{\rm OPE\ 0}\approx 3\times 10^{-29}\ {\rm cm}^2/{\rm sr}\quad{\rm at}\quad k\approx 5M\approx 5\ {\rm BeV}, \tag{28}$$

which may be compared with the corresponding cross section at this energy from the diffraction channel

$$\left(\frac{d\sigma}{d\Omega}\right)_{\rm Diffraction}\approx\left(\frac{g_{\omega\pi\rho}{}^2}{4\pi}\right)\left(\frac{g_{\gamma\pi\omega}{}^2}{4\pi}\right)\times 10^{-26}\ {\rm cm}^2/{\rm sr}$$

$$\approx 10^{-29}\ {\rm cm}^2/{\rm sr}\ \text{according to (11) and (12)};$$

$$\approx 3\times 10^{-28}\ {\rm cm}^2/{\rm sr}\ \text{according to (13) and (15)}. \tag{29}$$

To disentangle the one-π exchange and diffraction amplitudes, which do not interfere with one another because of the pseudoscalar coupling of the pion to the nucleon, one can compare ρ^0 with ρ^+ photoproduction to which the diffraction cannot contribute. Both mechanisms lead to transversely polarized ρ mesons in the forward direction. At higher energies the forward diffraction cross section wins out over the one-π exchange as (15) increases with k^2 whereas (27) is falling as $1/k^2$.

We may also compare electron or muon-pair production through a virtual π exchange with ordinary pair production and with the diffraction mechanism. The mechanism is shown by the Feynman diagram, Fig. 13. Comparing the cross section for the case of sym-

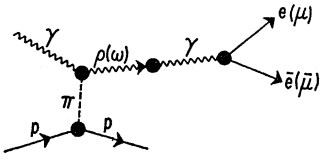

FIG. 13. One-pion exchange ρ^0's subsequently decaying into lepton pairs.

metric pairs as in Eq. (20) we find,

$$\frac{d\sigma_{\rho,\omega}}{d\sigma_{\text{Bethe-Heitler}}}=\left(\frac{3}{1280}\right)\left(\frac{s^2}{M^2m_\rho{}^2}\right)\frac{|t|}{(|t|+m_\pi{}^2)^2}\left(\frac{g_{\pi NN}{}^2}{4\pi}\right)\left(\frac{\Gamma_{\rho\to\pi\gamma}}{m_\rho}\right)\left|\frac{(4\pi)^{1/2}}{\gamma_\rho}\frac{m_\rho{}^2}{s-m_\rho{}^2+i\Gamma_\rho m_\rho}+\frac{g_{\gamma\pi\omega}}{g_{\gamma\pi\rho}}\frac{(4\pi)^{1/2}}{\gamma_\omega}\frac{m_\omega{}^2}{s-m_\omega{}^2+i\Gamma_\omega m_\omega}\right|^2$$

$$\approx 10^{-3}\times\left|\frac{(4\pi)^{1/2}}{\gamma_\rho}\frac{m_\rho{}^2}{s-m_\rho{}^2+i\Gamma_\rho m_\rho}+\frac{g_{\gamma\pi\omega}}{g_{\gamma\pi\rho}}\frac{(4\pi)^{1/2}}{\gamma_\omega}\frac{m_\omega{}^2}{s-m_\omega{}^2+i\Gamma_\omega m_\omega}\right|^2. \quad (30)$$

Because of the pseudoscalar coupling of the pion to the nucleon the amplitude of the one-pion-exchange model of $\rho(\omega)$ production does not interfere with the Bethe-Heitler amplitude.

For process (24) we express the πNN^* vertex directly in terms of the 33 resonance cross section as in Ref. 15. In that case we find in the lab system

$$\left(\frac{d\sigma}{d\Omega}\right)_{\text{lab},N^*}=\frac{3}{2\pi^2}\left(\frac{\Gamma_{\rho,\omega\to\pi\gamma}}{m_{\rho,\omega}}\right)\left[\frac{|t|+m_{\rho,\omega}{}^2}{|t|+m_\pi{}^2}\right]^2\times\left(\frac{p}{k}\right)\frac{E_R\Gamma_R}{m_{\rho,\omega}{}^2}\sigma_R\{1,\tfrac{2}{3},\tfrac{1}{3}\} \quad (31)$$

where Γ_R = width of 33 resonances $\approx m_\pi$, σ_R = 33 cross section $\approx$ 200 mb, E_R = pion energy necessary to excite 33 resonance $\approx$ 300 MeV and $\{1,\frac{2}{3},\frac{1}{3}\}$ are the isotopic factors for ρ^-, ρ^0, and ρ^+ production, respectively.

Alternatively, the cross section can be determined treating the N^* as a $\frac{3}{2}$ particle with a coupling constant determined from the known width of the 33 resonance. Following this procedure we find for process (24)

$$\left(\frac{d\sigma}{d\Omega}\right)_{\text{lab},N^*}=\left(\frac{3p^2}{2k^2}\right)\frac{1}{B_2m_{\rho,\omega}}\left(\frac{\Gamma_{\rho,\omega\to\pi\gamma}}{m_{\rho,\omega}}\right)\left(\frac{\Gamma_RM^{*2}}{q_0{}^3}\right)\times\frac{[|t|+(M^*-M)^2][|t|+(M^*+M)^2]}{(M+M^*)^2M^2M^{*2}}\{1,\tfrac{2}{3},\tfrac{1}{3}\}, \quad (32)$$

where B_2 is determined from B_1 in Eq. (26) by replacing $m_{\rho,\omega}{}^2$ with $(m_{\rho,\omega}{}^2+M^2-M^{*2})$, M^* is the 33-isobar mass; p, M and k are as before. The quantity q_0 is the momentum of the pion (or nucleon) from an N^* decaying at rest and numerically

$$\tfrac{3}{2}\Gamma_RM^{*2}/q_0{}^3\approx 26.$$

In the limit of $|t|=m_\pi{}^2$ Eqs. (31) and (32) are approximately equal. However, in the physical region Eq. (32) can be considerably larger than Eq. (31).

In the forward direction Eq. (31) yields for ρ^0 production, say,

$$\left(\frac{d\sigma}{d\Omega}\right)_{0^0,N^*}=\left(\frac{\Gamma_{\rho\to\pi\gamma}}{m_\pi}\right)\left(\frac{3m_\rho}{\pi^2m_\pi}\right)\sigma_R\frac{m_\pi{}^4}{(|t_{\min}|+m_\pi{}^2)^2}. \quad (33)$$

In general $|t_{\min}|$ is small compared to $m_\pi{}^2$ only at very high energies. For example, with $k=5M$, $|t_{\min}|=6.4\,m_\pi{}^2$. Using the value[10] of 0.5 MeV for $\Gamma_{\rho\to\pi\gamma}$ we find from Eq. (33) for ρ production at $k=5M$,

$$\left(\frac{d\sigma}{d\Omega}\right)_{0^0,N^*}=10^{-29}\text{ cm}^2/\text{sr}$$

which is comparable to Eq. (28) for process (23) even though one has the γ_5 coupling there. This is because $|t_{\min}|$ is larger for process (24) than (23). At higher energies the inelastic process (24) dominates over (23) since Eq. (27) decreases with increasing energy as $1/k^2$, whereas Eq. (33) increases as $|t_{\min}|$ decreases with $1/k^2$.

IV. COULOMB PRODUCTION OF VECTOR MESONS

In view of these large numbers as well as the intrinsic interest in the nature of vector boson couplings it is desirable to have an independent direct measure of $\Gamma_{\rho\pi\gamma}$. For example, the chain of reasoning in Gell-Mann *et al.*[2] leads to a significantly smaller decay width as noted earlier. We therefore propose a permutation of lines in Fig. 8 leading to conversion of a π into a ρ meson in the Coulomb field of a nucleus, as illustrated in Fig. 14.

$$\pi^\pm+Z\to\rho+Z.$$

The related processes of Coulomb production of π's and η's from incident photons have been considered by Primakoff and by Andersen, Halprin, and Primakoff,[16] and this mechanism has also been discussed recently by Pomeranchuk and Shmushkevich, Good, and Walker, and Barmin *et al.*[17] We confine our remarks here to

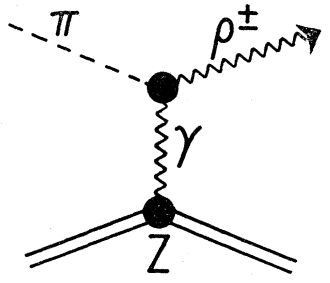

FIG. 14. Coherent production of ρ by π in the Coulomb field of a nucleus of charge Z.

[15] S. D. Drell, Phys. Rev. Letters **5**, 278 (1960).

[16] H. Primakoff, Phys. Rev. **81**, 899 (1951); C. Andersen, A. Halprin, and H. Primakoff, Phys. Rev. Letters **9**, 512 (1962).

[17] M. Good and W. Walker, Phys. Rev. **120**, 1855 (1960); I. Pomeranchuk and I. Shmushkevich, Nucl. Phys. **23**, 452 (1961); V. Barmin, Yu. Krestnikov, E. Kuznetsov, A. Meshkovskii, Yu. Nikitin, and V. Shebanov, in *Proceedings of the International Conference on High Energy Physics*, edited by J. Prentki (CERN, Geneva, 1962), p. 199. Our calculation for the Coulomb production is a factor of 2 larger than that of Pomeranchuk and Shmushkevich.

charged ρ production from charged π mesons as experimentally observable. In principle the same formulas are obtained for ρ^0 and ω^0 production from π^0's and indeed this latter process may be observable as a Z^2 contribution to ρ^0 and ω^0 production cross sections due to conversion in a final state interaction of emerging π^0's in the Coulomb field of the target nucleus.

For high-energy incident-charged pions the momentum transfer to the nucleus can be small enough so that the conversion of a charged pion into a ρ can occur coherently in the Coulomb field. For ρ's produced in the near forward direction this condition is achieved when

$$|t_{\min}|^{1/2}=(m_\rho^2/2E_\pi)<R_z^{-1},$$

where E_π is the incident laboratory pion energy and R_z is the radius of the nucleus of charged Z.

The differential cross section in the laboratory frame for ρ's produced at angle θ for this process is readily expressed in terms of the partial decay width $\Gamma_{\rho\to\pi\gamma}$ and the electromagnetic form factor of the nucleus $F(t)$ as

$$\left(\frac{d\sigma}{d\Omega}\right)_{Z,\text{lab}}=24Z^2\alpha F(t)\left(\frac{\Gamma_{\rho\to\pi\gamma}}{m_\rho}\right)\frac{1}{m_\rho^2}\times\frac{E_\pi^2 p_\rho^2\sin^2\theta}{[m_\rho^2-2E_\pi E_\rho(1-\beta\cos\theta)]^2},\quad(34)$$

where we have neglected terms proportional to the pion mass and where $\beta^2=1-m_\rho^2/E_\rho^2$. The form factor $F(t)$ is normalized so that $F(0)=1$ and, as usual, $\alpha=1/137$ is the fine structure constant. For small angles Eq. (34) becomes

$$\left(\frac{d\sigma}{d\Omega}\right)_{Z,\text{lab}}=Z^2\alpha F(t)\left[\frac{24\Gamma_{\rho\to\pi\gamma}}{m_\rho}\right]\frac{1}{m_\rho^2}\frac{\theta^2}{[\theta^2+m_\rho^4/4E_\pi^4]^2}.\quad(35)$$

This $1/\theta^2$ behavior of the cross section at small angles is familiar from the scattering of a magnetic dipole such as a neutron in a Coulomb field. In the present case, the $\pi\rho\gamma$ vertex [Eq. (4)] has the form which reduces at low-momentum transfers to a magnetic dipole interaction. Equation (35) has a sharp maximum at an angle $\theta=m_\rho^2/2E_\pi^2$. At this angle the differential cross section becomes

$$\left(\frac{d\sigma}{d\Omega}\right)_{Z,\max}=Z^2\alpha\left[\frac{24\Gamma_{\rho\to\pi\gamma}}{m_\rho}\right]\left(\frac{E_\pi}{m_\rho}\right)^4\frac{1}{m_\rho^2},\quad(36)$$

where we put $F(t)\approx 1$. That this is a very large cross section can be seen by considering an example of a 10-BeV pion beam incident on an aluminum target, in which case Eq. (36) becomes

$$\left(\frac{d\sigma}{d\Omega}\right)_{Z=13,\max;\ E_\pi=10\text{BeV}}=0.55\left(\frac{10^3\Gamma_{\rho\to\pi\gamma}}{m_\rho}\right)\text{b/sr}.$$

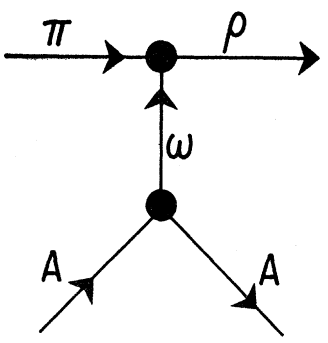

FIG. 15. Coherent production of ρ by π via ω exchange on nucleus of mass number A.

Again estimating $\Gamma_{\rho\to\pi\gamma}\approx 0.5$ MeV as in Eq. (15), we find a cross section at the maximum angle of 0.4 b/sr.

The ρ mesons produced in the Coulomb field will be transversely polarized for all production angles; hence, in the ρ rest system the decay angular distribution of pions will be of the form $\sin^2\theta_\pi$ where θ_π is the angle between pion momentum and ρ direction.

Since the π and ρ mesons both have unit isospin the possibility arises of an interfering coherent production of the ρ by the π in a complex nucleus via purely strong interactions. This interfering process would not be expected to have the sharp angular distribution of the Coulomb production since the denominator in Eq. (34) is replaced by the square of the ω propagator, $\approx(1/m_\omega^2)^2$, but it might also contribute a large cross section. In order to estimate roughly the relative magnitudes of the strong production to the Coulomb production, we consider a model in which the ρ is peripherally produced with a one-ω-exchange pole as shown in Fig. 15. Using Eq. (11) for the $\pi\rho\omega$ coupling constant and assuming the ω-nucleon coupling constant to be of order unity, the ratio of the Coulomb to the strong production amplitude in the forward direction is roughly

$$\frac{Z}{A}\left[\frac{\alpha}{(m_\rho^2/2E_\pi)^2}\right]m_\omega^2\approx\frac{4\alpha E_\pi^2}{m_\rho^2}(Z/A).\quad(37)$$

For pion energies greater than 10 BeV, the above estimate indicates that, in the region of its maximum, the Coulomb production should be larger than the coherent strong production.

In any case Eq. (37) is undoubtedly a gross overestimate of the $\pi\rho\omega$ contribution. From a Regge-pole analysis of the decreasing magnitude of the difference of $\bar{p}p$ and pp total cross sections at high energy, one is led to a reduction of the ω propagator at zero momentum transfer by a factor $\approx(E/M)^{-0.6}<\frac{1}{3}$. Also for the pp elastic cross section one finds by perturbation theory a ratio of the real amplitude at forward scattering angles due to ω exchange to the imaginary amplitude determined from observed total cross sections by the optical theorem of $\text{Re}/\text{Im}\approx 4\pi(g_{\omega NN}^2/4\pi)M^2/m_\omega^2$ where M is the nucleon mass. Since this ratio appears experi-

mentally to be small at high energies, we conclude that $g_{\omega NN}^2/4\pi$ can at most be $\approx 10^{-1}$ and may be smaller. It is therefore unlikely that the coherent ω-exchange contribution buries the Coulomb production. Detection of it by observing its broad angular distribution will be interesting in its own right as a measure of $g_{\omega NN}$.[11]

In the laboratory system the energy and angular distribution of the decay charged pion of momentum p and energy E has the form

$$d^3p\left[\frac{a}{(a^2-b^2)^{1/2}}-1\right]\frac{p}{E}, \tag{38}$$

where

$$a=[E_\pi-(E_\pi^2-m_\rho^2)^{1/2}]^2+2E_\pi(E_\pi^2-m_\rho^2)^{1/2}\times[1-\cos\theta_0\cos\theta],$$

$$b=2E_\pi(E_\pi^2-m_\rho^2)^{1/2}\sin\theta_0\sin\theta,$$

$$\cos\theta_0=\left[\frac{E_\pi E}{p(E_\pi^2-m_\rho^2)^{1/2}}-\frac{m_\rho^2}{2p(E_\pi^2-m_\rho^2)^{1/2}}\right].$$

In the exact forward direction Eq. (38) vanishes for all energies E. For small angles Eq. (38) becomes

$$d^3p\left\{\frac{\frac{m_\rho^4}{4E_\pi^4}+\theta_0^2+\theta^2}{\left\{\frac{m_\rho^8}{16E_\pi^8}+\frac{m_\rho^4}{4E_\pi^4}(\theta^2+\theta^2)+(\theta_0^2-\theta^2)^2\right\}^{1/2}}-1\right\},$$

where terms of order m_π have been neglected.

If observed, Coulomb production will serve as an interesting check on the interpretation of the experiment of McLeod *et al.*[10] which suggested the somewhat surprisingly large width $\Gamma_{\rho\to\pi\gamma}$. It will also provide a valuable input number for the various chains of arguments presented in Refs. (1) and (2) and above suggesting cross section variations of interest to high-energy photon accelerators.

Similar calculations can also be applied to the process of Coulomb conversion of a K to a K^* meson. The smaller mass difference, $M_{K^*}-M_K=390$ MeV, makes the minimum momentum transfer $[(M_{K^*}^2-M_K^2)/2E]$ approximately the same as the ρ case for a given incident energy. At this time we have no clue, however, as to the $K^*\to K+\gamma$ decay width which may possibly be best determined by a study of its Coulomb production. (Note that in the Unitary Symmetry scheme the coupling constant for $\rho^+\to\pi^+\gamma$ is equal to the coupling constant for $K^{*+}\to K^+\gamma$.)

V. VECTOR BOSON EXCHANGES

Returning to photoproduction amplitudes we consider briefly the possibility of photoproducing a vector particle by absorption on its current as shown in Fig. 16.

The similar case of the particle pair being a $\pi^+\pi^-$ pair is well known from studies on single-pion photo-

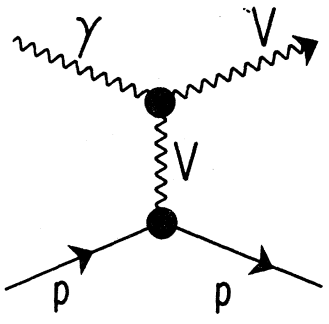

FIG. 16. Photoproduction of a vector meson via exchange of the antivector meson.

production. Because pions are spin-zero particles these cross sections are proportional to $\sin^2\theta$, where θ is the angle between the produced pion and the incoming photon. The existence of strongly interacting bosons of spin unity such as the ρ, ω, and K^* mesons leads one to entertain the possibility that these particles are also photoproduced in a similar manner as in Fig. 16. If these vector mesons have a magnetic moment, then the $\sin^2\theta$ factor present in the pion case will be absent; hence, even though the propagator for the exchange particle will have a larger mass, the cross sections in the vicinity of the forward direction may be as large as the case when $V\bar{V}$ is a pion pair.[15]

Since photons are odd under charge conjugation the only possibilities for $V\bar{V}$ among ρ, ω, and K^* are

$$\rho^+\rho^-;\quad K^{*+}K^{*-};\quad K^{*0}\bar{K}^{*0}.$$

A numerical estimate for the cross section even for two-body final states such as

$$\gamma+p\to\rho^++n, \tag{39a}$$

$$\gamma+p\to K^*+\Lambda(\Sigma^0) \tag{39b}$$

involves knowing, in addition to the charge, the magnetic moment, the quadrupole moment of the vector mesons and their coupling with baryons which are all unknown. Here we consider only the charge coupling of vector mesons to baryons which will dominate for small momentum transfers unless the magnetic coupling constant is very large compared to the charge coupling constant.

For the interaction vertex of a photon at a vector boson line as in Fig. 17, we write[18]

$$\Gamma_{\mu\alpha\beta}=eF_1(p_1+p_2)_\mu g_{\alpha\beta}+e(F_1+\mu_V F_2)(p_2-p_1)_\lambda\times(g_{\lambda\beta}g_{\mu\alpha}-g_{\lambda\alpha}g_{\mu\beta})+\frac{QF_3}{2m^2}\{k_\alpha[p_2\cdot kg_{\beta\mu}-p_{2\mu}k_\beta]+k_\beta[p_1\cdot kg_{\alpha\mu}-p_{1\mu}k_\alpha]\}, \tag{40}$$

where the kinematics are as drawn, and where e is the charge $(1+\mu_V)$ is the static g factor and (μ_V+Q) is the static electric quadrupole moment.

[18] See also V. Glaser and B. Jakšić, Nuovo Cimento 5, 1197 (1957).

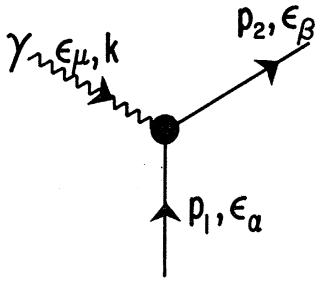

FIG. 17. The photovector meson vertex. The photon has polarization ϵ_μ and momentum k; the initial and final vector mesons have polarizations $\epsilon_1, \epsilon_2 \rightarrow \epsilon_\alpha, \epsilon_\beta$.

It is possible to show that all other terms except the pure magnetic moment interaction between photons and a pair of vector mesons are either proportional to $\sin^2\theta$ or vanish at the pole $|t|=+m_\rho^2$, and hence in the spirit of the one-meson pole approximation, we consider only the magnetic moment coupling between photon and vector meson. With these assumptions we find for process (39a) the cross section in the laboratory system

$$\left(\frac{d\sigma}{d\Omega}\right)_{V,\text{lab}}=\alpha\left(\frac{g_{\rho NN}^2}{4\pi}\right)\frac{1}{8M^2}\left(\frac{p}{k}\right)^2\frac{(1+\mu_V)^2}{m_\rho^2[|t|+m_\rho^2]^2}\times\left\{(2m_\rho^2+|t|)Mk(2M\epsilon-m_\rho^2)-\frac{(|t|-m_\rho^2)(2M^2-|t|)}{4}\right\},\quad(41)$$

where $(1+\mu_V)$ is the total magnetic moment of the charged vector boson, i.e., $\mu_V=0$ corresponds to a g factor of unity for a charged ρ interacting with a constant magnetic field, and where $\epsilon=(p^2+m_\rho^2)^{1/2}$.

In the forward direction (41) becomes

$$(d\sigma/d\Omega)_{V,00}=\alpha(g_{\rho NN}^2/4\pi)(1+\mu_V)^2\times(0.7)10^{-27}\text{ cm}^2/\text{sr}.\quad(42)$$

A value of $g_{\rho NN}^2/4\pi$ of unity yields a differential cross section comparable to the case of one-pion exchange as calculated in (28). However, by comparing the experimental pp-pn cross sections as well as the $\pi^-p-\pi^+p$ cross sections with the perturbation calculation using the one-ρ exchange we find a considerable reduction from unity of the coupling constant $g_{\rho NN}^2/4\pi$. Since the one-ρ exchange does not interfere with the one-pion exchange the charged-ρ production will be the sum of Eqs. (28) and (42).

To the extent that the baryon mass differences are neglected (which is a good approximation for photon energies above 3 BeV) Eq. (41) may be applied to process (39b) with m_ρ replaced by m_{K^*} and $g_{\rho NN}$ replaced by g_{K^*NY}.

VI. SECONDARY BEAMS

The various mechanisms discussed here may be considered and compared as candidates for producing secondary pion (or K-meson beams) at electron accelerators. Both the diffraction mechanism of Sec. II and the one-pion-exchange amplitude in Sec. III lead to neutral ρ^0 mesons which decay to a $\pi^+-\pi^-$ pair, each of which is readily detected in a coincidence experiment. The differential cross sections for the π^+ and π^- to emerge with energies ω_+ and $\omega_-=k-\omega_+$ in solid angle intervals $d\Omega_+$ and $d\Omega_-$ about θ_+ and θ_-, respectively, are readily computed. With neglect of target recoil, corresponding to low momentum transfers $|t|<m_{\rho,\omega}^2$, we find in the limit $m_\pi\rightarrow 0$ for the OPE case

$$\frac{d\sigma}{d\Omega_+d\Omega_-}=\left(\frac{3}{\pi}\right)\left(\frac{k^2}{k^2-m_\rho^2}\right)\left\{\frac{(1-\cos\theta_+)(1-\cos\theta_-)}{(1-\cos\theta_{+-})^3}\times\frac{1}{[1-2m_\rho^2/k^2(1\pm\cos\theta_{+-})]^{1/2}}\right\}\left(\frac{d\sigma}{d\Omega}\right)_{\text{lab}},\quad(43)$$

where k is the incident photon energy and θ_{+-} is the angle between the π^+ and π^- mesons. For $\cos\theta_{+-}>1-2m_\rho^2/k^2$ the positive sign in the square root of Eq. (43) is taken, and for $\cos\theta_{+-}<1-2m_\rho^2/k^2$ the negative sign is taken. The expression for $(d\sigma/d\Omega)_{\text{lab}}$ is as given by Eqs. (25) or (27). For excitation of the 33 resonance in the one-π-exchange process the only significant change at high energies is the replacement of k^2 by $(k+M-M^*)^2$ in the square root and the use of Eqs. (31), (32), or (33) for $(d\sigma/d\Omega)_{\text{lab}}$. More generally for the process

$$\gamma+p\rightarrow\rho^0+(\text{others})\quad\searrow\ \pi^++\pi^-$$

one finds in the limit of small energy loss to the recoiling target in the OPE approximation

$$\left(\frac{d\sigma}{d\Omega_+d\Omega_-}\right)_{\text{inelas.}}=\left(\frac{d\sigma}{d\Omega_+d\Omega_-}\right)_{\text{elas.}}\times\left\{\frac{4M^2}{\pi g^2}[\sigma_{\pi N}^{\text{tot}}(k-\epsilon_+-\epsilon_-)]\frac{k-\epsilon_+-\epsilon_-}{|t|}d\epsilon_\pm\right\},\quad(44)$$

where $d\sigma/d\Omega_+d\Omega_{-\text{elas.}}$ is given in Eq. (43) with the $k^2\rightarrow(k+M-M^*)^2$ as indicated above and where ϵ_+, ϵ_- are the laboratory energies of the π^+ and π^-, respectively.

If one integrates over the variables of one of the pions and asks instead for the cross section to produce a single pion in a given momentum and solid angle interval there results from Eq. (25) in the limit of no target recoil

$$\left(\frac{d\sigma}{d\Omega d\epsilon}\right)=\left(\frac{g_{\pi NN}^2}{4\pi}\right)\left(\frac{3.6\times10^{-27}\text{ cm}^2}{m_\rho}\right)\left(\frac{\epsilon}{m_\rho}\right)\theta^2\times\left[1+\frac{m_\rho^2-2m_\pi^2-\theta^2k\epsilon}{[\{m_\pi^2+k^2(\theta+\theta_0)^2\}\{m_\pi^2+k^2(\theta-\theta_0)^2\}]^{1/2}}+\frac{m_\pi^2[k\epsilon\theta^2+m_\pi^2-m_\rho^2][m_\pi^2+k^2(\theta^2+\theta_0^2)]}{[\{m_\pi^2+k^2(\theta+\theta_0)^2\}\{m_\pi^2+k^2(\theta-\theta_0)^2\}]^{3/2}}\right],\quad(45)$$

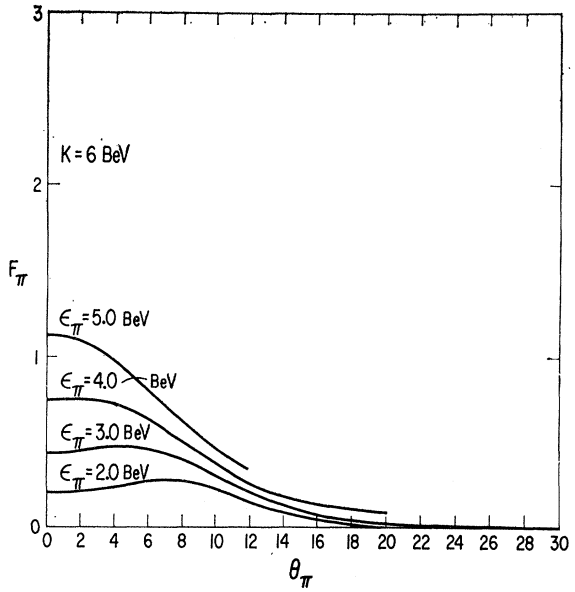

FIG. 18. Function F_π in Eq. (46) for π photoproduction via the ρ-exchange current as in Fig. 16.

where ϵ and θ are the energy and angle of the pion with respect to the incident photon, k is the incident photon energy and

$$\cos\theta_0=[(k/p)-m_\rho^2/2\epsilon p], \quad \text{with} \quad p^2=k^2-m_\rho^2.$$

This predicts an angular distribution of high-energy pions distributed over a cone of opening angle $\approx m_\rho/k$. The corresponding pion flux from photoproduction on the pion current where the final ρ of Fig. 12 is replaced by a charged pion (and N^* represents any final state)[15] is concentrated in a narrower cone of opening angle $\approx m_\pi/k$ and appears to dominate at such forward angles. For example, the ratio of the pion flux from the above process to pions from ρ decay as given by Eq. (45) at $\theta_\pi=m_\pi/k$ is

$$R\approx\frac{\alpha(g^2/4\pi)^{-1}}{8\pi^2(9\Gamma_{\rho\to\pi\gamma}/m_\rho)}\frac{m_\rho^2M^2}{m_\pi^4}(k-\epsilon)k\sigma_{\pi N}(k-\epsilon)$$
$$\approx 200k(k-\epsilon)\sigma_{\pi N}(k-\epsilon)\gg 1$$

at high energies. Similar conclusions are suggested by comparing the diffraction production and the inelastic production with the above direct photon pion current interaction.

Finally we may compare with the contribution from the ρ exchange current Eq. (41) which, for a finite g factor of the $\rho^\pm$, escapes the $\sin^2\theta$ suppression of the other mechanisms in the forward direction. In this case we find for pion energies $\epsilon_\pi>\frac{1}{2}k$

$$\frac{d^2\sigma}{d\Omega_\pi d\epsilon_\pi}=\frac{(1+\mu_V)^2}{\pi}\left(\frac{g_{\rho NN}{}^2}{4\pi}\right)\left(\frac{\epsilon_\pi{}^4}{kM^3}\right)$$
$$\times\left\{\frac{m_\rho{}^2}{8\epsilon_\pi{}^2}+\sin^2\theta_{\pi/2}\left[1-\frac{k}{2\epsilon_\pi}\right]\right\}F_\pi(\theta_\pi,\epsilon_\pi)$$
$$\times 10^{-27}\ \text{cm}^2/\text{BeV-sr}. \quad (46)$$

The function F_π is in the neighborhood of unity for forward angles and is shown for a few cases in Fig. 18. The ratio to the beam from one-π exchange as calculated in Ref. 15 is given at $\theta_\pi\approx m_\pi/k$ by

$$R_{\rho/\pi}\approx(1.5\pi)(m_\pi/M)^4\left[\frac{(1+\mu_V)^2(g_{\rho NN}{}^2/4\pi)}{\alpha}\right.$$
$$\left.\times\left(\frac{\epsilon_\pi}{k-\epsilon_\pi}\right)\left(\frac{m_\pi{}^2}{\sigma_{\pi N}(k-\epsilon_\pi)}\right)\right].$$

In view of the unknown magnetic moment of the charged ρ and coupling constant $g_{\rho NN}{}^2/4\pi$ this ratio is undetermined. An appreciable ρ current contribution would appear as a contribution to a charged pion flux spread over an angular cone of opening angle m_ρ/k but not leading to charged pion pairs as in Eqs. (43), (44), and (45) since the ρ here must be charged.

All the above considerations may be applied to K production at high energies if we make the correspondence $\pi\to K$ and $\rho\to K^*$. Measurement of the Coulomb production of K^* mesons as in Sec. IV will indicate whether the (γKK^*) interaction may play a dominant role in K beam production in photon machines. In view of the larger K mass which pushes the pole in the one K exchange amplitude much further from the physical region than for one-π exchange we expect that the K^*-current contribution may play a dominant role as a K-production mechanism. Whether the anomalous thresholds in the γK^*K^* vertex significantly reduce this amplitude for virtual exchanged K^*'s of $\approx$ zero mass is an open question.